Available online at www.sciencedirect.com

ScienceDirect

Thermochimica Acta 462 (2007) 38–44

thermochimica acta

www.elsevier.com/locate/tca

Tuning phase diagram of ternary polymer blends by tacticity

Wen-Ping Hsu*, Wei-Chun Chiu

Department of Chemical Engineering, National United University, Kung-Ching Li, Miao-Li 36003, Taiwan, ROC

Received 27 March 2007; received in revised form 7 June 2007; accepted 10 June 2007
Available online 20 June 2007

Abstract

Previously, a ternary blend consisting of poly(vinyl phenol) (PVPh), poly(vinyl cinnamate) (PVCN) and poly(methyl methacrylate) (PMMA) was reported to exhibit a closed-loop behavior of immiscibility. In that study, PMMA was atactic PMMA and three binary pairs of PVPh, PVCN and PMMA were all miscible. In this article, isotactic and syndiotactic PMMAs (designated as iPMMA and sPMMA) were used to replace atactic PMMA to blend with PVPh and PVCN. For iPMMA ternary blends, the ternary phase diagram was found to demonstrate a closed-loop immiscibility behavior similar to the previous study. However, a completely miscible region was observed in sPMMA ternaries even though sPMMA and PVCN were found to be not miscible.

Keywords: Phase diagram; Ternary polymer blends; Tacticity

1. Introduction

With the increasing application of multicomponent polymers [1,2], much interest has been directed toward ternary polymer blends recently. Since the early works of Scott and Tompa [3,4], most studies on the ternary polymer blends have been centered on the concept that polymer A, which is miscible with both polymers B and C, can compatibilize the immiscible binary pair B and C [5–8]. When all three binary pairs are miscible, a completely homogeneous ternary is possible [9]. However, differences in the interaction parameters of the binary system, the so-called "$\Delta\chi$ effect", can result in phase separation.

The phase relationships for ternary mixture where one component is solvent and the other two polymers have been described by Scott and Tompa [3,4] using the lattice theory of Flory and Huggins. Robard et al. [10] have demonstrated the existence of the $\Delta\chi$ effect in a ternary mixture of poly(styrene), poly(vinyl methyl ether) and chloroform. A distinguished feature in this ternary is the closed-loop region of immiscibility. The extension of the Flory–Huggins theory to ternary polymer blends has been conducted by Hsu and Prausnitz [11]. The effect of the asymmetry in the interaction parameters as well as the difference in molecular weight of the coexistence curves has been simulated. Su and Fried [12] also used the Flory–Huggins theory to compute spinodal curves and critical points for different interaction parameters, thus providing useful predictions in the phase diagrams of ternary systems.

In our previous study [13], a ternary polymer blend of poly(vinyl phenol) (PVPh), poly(vinyl cinnamate) (PVCN) and poly(methyl methacrylate) (i.e. atactic PMMA) was investigated calorimetrically. The binary pairs of this ternary all exhibited miscible behavior. However, a closed-loop behavior of immiscibility in the ternary phase diagram was observed. The reason for this observation is likely because of stronger PMMA/PVPh interaction than PMMA/PVCN interaction (the $\Delta\chi$ effect).

In this article, atactic PMMA (aPMMA) was replaced by isotactic or syndiotactic PMMA (iPMMA or sPMMA). A ternary blend of iPMMA(or sPMMA), PVPh and PVCN were prepared and measured by calorimetry. The results of iPMMA ternary were similar to previous aPMMA ternary study. All three binary pairs of iPMMA ternary were miscible. A closed-loop region of immiscibility was still observed but much smaller for iPMMA with approximately the same molecular weight as aPMMA. For iPMMA(1) with higher molecular weight and lower T_g (detail will be listed in Section 2), its ternary was found to exhibit larger immiscibility region than aPMMA ternary. However, for sPMMA ternary a completely miscible region of ternary phase diagram was detected even though sPMMA was not miscible with PVCN. The experimental results of

---

* Corresponding author. Tel.: +886 37 381571; fax: +886 37 332397.
E-mail address: mjkr.hsu@msa.hinet.net (W.-P. Hsu).

0040-6031/$ – see front matter © 2007 Elsevier B.V. All rights reserved.
doi:10.1016/j.tca.2007.06.005

calorimetry were presented in this article. Observation of phase diagram was expounded in terms of binary enthalpic interaction. The k value of the Gordon–Taylor equation was proven to be a good indicator of binary interaction. The results indicated tacticity of PMMA had a decisive effect on tuning its ternary phase diagram with PVPh and PVCN. To the best of our knowledge, these results of tacticity effect on ternary phase diagram were rare. In comparison with previous study of aPMMA ternaries [13], iPMMA or sPMMA with approximately the same molecular weight as aPMMA was shown mostly to demonstrate miscible behavior when blended with PVPh and PVCN.

2. Experimental

2.1. Materials

PMMA and PVPh were purchased from Polysciences, Inc., Warrington, PA. According to manufacturer information, the molecular weight of iPMMA (or sPMMA) was 100,000 g/mol about the same as aPMMA of previous study. iPMMA(1) with a M_w value of 300,000 g/mol was used to represent iPMMA with low T_g and obtained from Scientific Polymer Products, Inc. (Ontario, NY). The M_w values for PVPh were 9000–11,000 g/mol. PVCN also obtained from Scientific Polymer Products, Inc. had a M_w value of 100,000 g/mol.

2.2. Film preparation

Thin films of the following binary and ternary polymer blends were made by solution casting from tetrahydrofuran (THF) onto glass plates. The actual compositions of the binary and ternary blends are shown later in corresponding Tables and Figures. THF is reagent grade purchased from Riedel-deHaën, Germany. The final drying step for all the films took place in a vacuum oven at ca. 70 °C for about 24 h. The temperature at 70 °C was chosen to prevent PVCN from undergoing thermal cross-linking. Then the films were cooled to room temperature slowly by air to make as-cast samples. The as-cast samples were later used for DSC studies.

2.3. Differential scanning calorimetry (DSC)

Glass transition temperatures (T_gs) of the polymer blends were determined by a DuPont TA 2100 thermal analyzer. The scanning range for temperature was from 30 to 220 °C and a heating rate of 20 °C/min was used in every measurement. The experiments were often performed in two consecutive scans in the ambient environment of nitrogen gas at a flow rate of 20 ml/min. In the first thermal scan, the samples stayed at 220 °C for 2 min. Then the samples were cooled to 30 °C using a cooling rate of 20 °C/min. The mid-point of the specific heat jump of a second thermal scan was taken as the glass transition temperature. The cooling rate was proven to be fast enough to produce virtually the same results as quenching. ΔT_g is calculated as the difference between the onset and end points of the glass transition temperature region.

3. Results and discussion

Thermal scans of calorimetry were not shown for brevity. The calculated glass transition temperature data are presented in the following section.

3.1. PVPh/PMMA blends

Table 1 presents the glass transition temperatures (T_gs) of PVPh/PMMA blends. Single composition dependent T_g was detected in the blends indicating miscibility mostly in agreement with literature [14]. The only difference from literature is sPMMA was found to be miscible with PVPh in this article likely due to low PVPh molecular weight. Different T_g equations can be used to describe experimental results. In our case, the Gordon–Taylor equation [15] seemed to be applicable for different binary blends. The equation is as follows:

$$T_g = \frac{w_1 T_{g1} + k w_2 T_{g2}}{w_1 + k w_2} \tag{1}$$

where T_g is the glass transition temperature of a blend, T_{gi} and w_i are the glass transition temperature and the weight fraction of polymers i, respectively ($i = 1, 2$). k (originally a function of the cubic expansion coefficient and the specific volume) is commonly considered as an adjustable parameter. k values of 0.89, 1.93 and 0.22 were found to describe the T_g data in the order of PVPh/iPMMA(1), PVPh/iPMMA and PVPh/sPMMA blends approximately good. The T_{gG} values (estimated by putting T_gs of component polymers and corresponding k values into Eq. (1)) were listed in the middle column of Table 1. The k values can be used as an indicator of interaction. Therefore the strength of interaction can be arranged in the following order: PVPh/iPMMA > PVPh/iPMMA(1) > PVPh/sPMMA. The strength of interaction is qualitatively related to the Flory–Huggins interaction parameter. ΔT_g values of the afore-

Table 1
Glass transition temperatures of PVPh/PMMA blends

	T_g (°C)	T_{gG} (°C)	ΔT_g (°C)
PVPh/iPMMA(1)			
100/0	137.3	137.3	11
75.0/25.0	108.8	112.5	13
50.0/50.0	80.0	89.0	18
25.0/75.0	74.7	67.0	13
0/100	46.1	46.1	9
PVPh/iPMMA			
100/0	137.3	137.3	11
74.8/25.2	129.6	127.2	24
50.0/50.0	114.5	114.2	13
25.0/75.0	89.1	96.2	11
0/100	69.7	69.7	12
PVPh/sPMMA			
100/0	137.3	137.3	11
75.0/25.0	128.9	126.9	12
50.0/50.0	122.5	123.2	17
25.0/75.0	120.9	121.3	17
0/100	120.1	120.1	7

Table 2
Glass transition temperatures of PVCN/PMMA blends

	T_g (°C)	T_{gG} (°C)	ΔT_g (°C)
PVCN/iPMMA(1)			
100/0	76.7	76.7	12
74.7/25.3	75.0	75.3	12
50.0/50.0	71.2	72.9	10
25.0/75.0	70.1	75.3	11
0/100	46.1	46.1	9
PVCN/iPMMA			
100/0	76.7	76.7	12
75.0/25.0	75.0	75.7	11
50.0/50.0	74.8	74.4	12
25.1/74.9	72.9	72.6	13
0/100	69.7	69.7	12
PVCN/sPMMA			
100/0	76.7		11
74.9/25.1	76.4, 108.0		9, 10
50.0/50.0	75.0, 107.6		10, 11
25.0/75.0	70.2, 117.7		9, 8
0/100	120.1		10

mentioned blends are also tabulated in Table 1 and a slightly T_g broadening phenomenon was observed in few blend compositions.

3.2. PVCN/PMMA blends

The glass transition temperatures of PVCN/PMMA blends are given in Table 2. For PVCN/iPMMA(1) and PVCN/iPMMA blends, single T_g was observed demonstrating possible miscibility similar to PVCN/aPMMA blends [13]. For PVCN and iPMMA their T_g values are very close, the transparency of prepared films were used to insure their miscibility. The experimental T_g values of PVCN/iPMMA(1) and PVCN/iPMMA blends can be fitted by the Gordon–Taylor equation with k values of 7.1 and 2.05, respectively. The predicted T_{gG} values were also listed in Table 2. However, for PVCN/sPMMA blends two T_g values were observed indicating immiscibility. Judging from the two observed T_g values, sPMMA was almost insoluble in PVCN but PVCN was slightly soluble in sPMMA deduced from high T_g value depression.

3.3. PVPh/PVCN blends

Table 3 shows the glass transition temperatures of PVPh/PVCN blends. Single T_g fitted well by the Gordon–Taylor equation with a k value of 0.79 demonstrated miscible behavior. ΔT_g values of the aforementioned blends are also tabulated in Table 3 for reference and a slightly T_g broadening phenomenon was observed in mid-blend compositions.

Table 3
Glass transition temperatures of PVPh/PVCN blends

	T_g (°C)	T_{gG} (°C)	ΔT_g (°C)
PVPh/PVCN			
100/0	137.3	137.3	11
75.0/25.0	119.8	119.3	23
50.0/50.0	104.0	103.4	21
25.0/75.0	88.5	89.3	15
0/100	76.7	76.7	10

3.4. Ternary blends

The glass transition temperatures of the PVPh/iPMMA(1)/PVCN blends are tabulated in Table 4. There are five blend compositions showing two T_g values indicating immiscibility. ΔT_g values of the aforementioned blends are also tabulated in Table 4 for reference. For the purpose of illustrating the effect of PVPh addition, the T_g values of the ternaries with iPMMA(1)/PVCN weight ratios of (3/1, 1/1 and 1/3) taken from Table 4 were plotted in Fig. 1(a)–(c). Results of the corresponding binaries (PVPh/PVCN and PVPh/iPMMA(1) blends) were also included in Fig. 1 for comparison. For iPMMA(1)/PVCN (weight ratios 3/1) ternaries (in Fig. 1(a)), the 75% PVPh blend showed two T_g values indicating immiscibility. The two T_g values likely correspond to two phases. The low T_g phase is mainly composed of iPMMA(1) and PVCN. The main components of the high T_g (matched closely to the T_g of PVPh/PVCN blends) phase are PVPh and PVCN. The other two blend compositions in Fig. 1(a) exhibited single T_g demonstrating miscible behavior. In Fig. 1(b), the ternaries with iPMMA(1)/PVCN ratio 1/1 demonstrated two T_gs at 50% and 75% PVPh indicating immiscibility. The two T_g phase behavior was similar to the one in Fig. 1(a). The iPMMA(1)/PVCN (1/3) ternaries in Fig. 1(c) also showed two T_g values at the same PVPh compositions as Fig. 1(b). However, the location of the high T_g values are different.

The glass transition temperatures of the PVPh/iPMMA/PVCN blends are shown in Table 5. For iPMMA ternaries, the results are very different from iPMMA(1) ternaries. Only one of nine studied blend compositions exhibited two T_g values indicating immiscibility. The explanation for the difference between iPMMA and iPMMA(1) ternaries will be discussed later in the phase diagram and Fox equation section. ΔT_g values of the aforementioned blends are also listed in Table 5 for reference. Two blend compositions with 50% PVPh demonstrated slightly glass transition broadening phenomenon. For the purpose of illustrating PVPh addition effect, the T_g values of the ternaries with iPMMA/PVCN weight ratios of (3/1, 1/1 and

Table 4
Glass transition temperatures of PVPh/iPMMA(1)/PVCN blends

	T_g (°C)	ΔT_g (°C)
PVPh/iPMMA(1)/PVCN		
74.9/18.6/6.5	69.7, 120.6	10,16
75.0/12.5/12.5	71.4, 119.1	11,15
75.1/6.7/18.2	75.3, 110.8	11,13
50.0/37.5/12.5	74.8	10
50.2/12.6/37.2	72.7, 103.5	15,13
50.0/12.5/37.5	75.0, 107.0	15,13
25.1/56.5/18.4	80.2	16
25.1/37.9/37.0	81.1	13
25.2/18.4/56.4	88.6	12

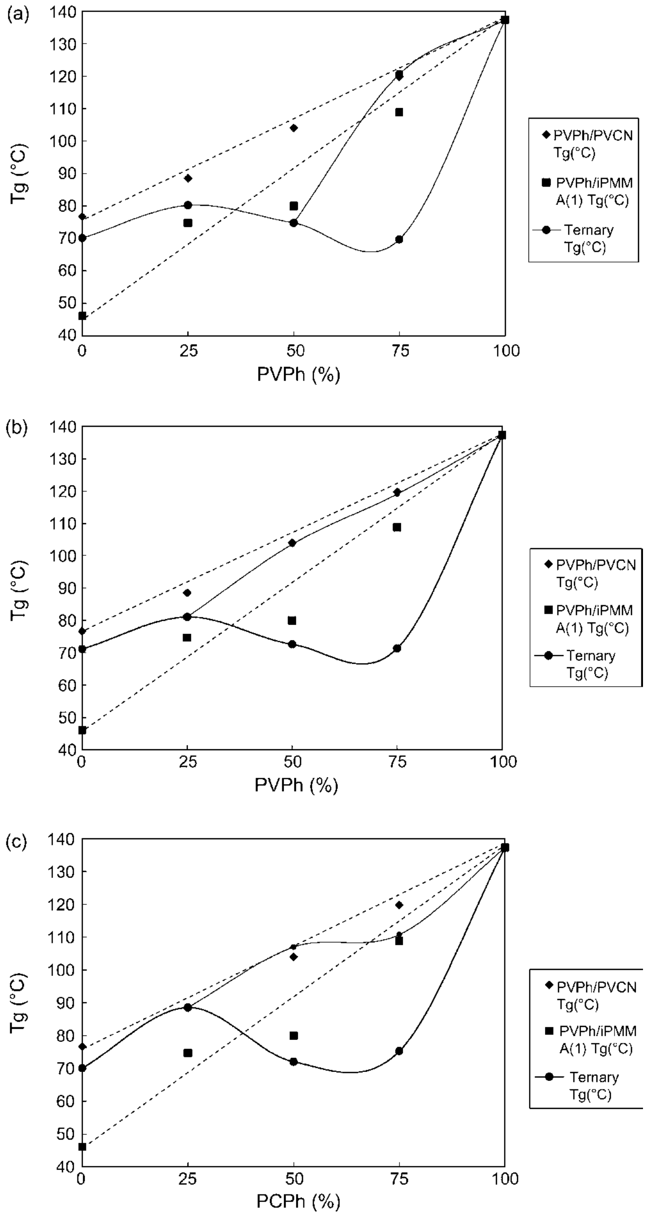

Fig. 1. (a) Change of T_g of the ternary blends with PVPh composition (iPMMA(1) /PVCN weight ratio = 3/1). (●) Data point, (♦) PVPh/PVCN blends, (■) PVPh/iPMMA(1) blends (curves drawn for viewing). (b) Change of T_g of the ternary blends with PVPh composition (iPMMA(1) /PVCN weight ratio = 1/1). (●) Data point, (♦) PVPh/PVCN blends, (■) PVPh/iPMMA(1) blends (curves drawn for viewing). (c) Change of T_g of the ternary blends with PVPh composition (iPMMA(1) /PVCN weight ratio = 1/3) (●) data point, (♦) PVPh/PVCN blends, (■) PVPh/iPMMA(1) blends (curves drawn for viewing).

1/3) taken from Table 5 were plotted in Fig. 2(a)–(c). Results of the corresponding binaries (PVPh/PVCN and PVPh/iPMMA blends) were also included in Fig. 2 for comparison. On the basis of observations in Fig. 4(a and b), the blends all showed one T_g indicating miscibility. For iPMMA/PVCN (weight ratio 3/1) ternaries, the T_g relation with two corresponding binaries demonstrated an interestingly S-shape behavior. However, for iPMMA/PVCN (1/1) ternaries the ternary T_g values are mostly higher than those of two corresponding binaries. In iPMMA ternary, only one immiscible composition with two T_g values occurred in the iPMMA/PVCN(1/3) ternary with 75% PVPh (Fig. 2(c)). At this immiscible composition, the blend probably phase separated into the high T_g phase composed mainly of PVPh and the low T_g phase consisting of PVCN and iPMMA components.

Table 5
Glass transition temperatures of PVPh/iPMMA/PVCN blends

	T_g (°C)	ΔT_g (°C)
PVPh/iPMMA/PVCN		
75.2/18.6/6.2	129.6	10
75.0/12.5/12.5	135.2	10
75.1/6.6/18.3	71.2, 130.6	12, 16
50.0/37.6/12.4	111.9	13
49.9/25.3/24.8	107.5	30
50.2/12.6/37.2	102.6	32
24.7/56.5/18.8	81.3	12
25.2/37.8/37.0	97.3	10
25.0/18.5/56.5	93.1	15

The glass transition temperatures of the PVPh/sPMMA/PVCN blends are given in Table 6. For sPMMA ternaries, single T_g value was observed for the nine studied blend compositions demonstrating miscible behavior. ΔT_g values of the aforementioned blends are also tabulated in Table 6 for reference. For the purpose of illustrating the effect of PVPh addition, the T_g values of the ternaries with sPMMA/PVCN weight ratios of (3/1, 1/1 and 1/3) taken from Table 6 were plotted in Fig. 3(a)–(c). Results of the corresponding binaries (PVPh/PVCN and PVPh/sPMMA blends) were also included in Fig. 3 for reference. In Fig. 3(a), single T_g value of the ternaries of with sPMMA/PVCN weight ratio 3/1 is always higher than the average of two corresponding binaries. For the compositions with 50% or 75% PVPh, the single T_g is even higher than the high T_g of corresponding binaries. The reason for this observation is probably due to more binary interactions or some ternary interactions. For the ternaries in Fig. 3(b) (sPMMA/PVCN weight ratio 1/1), the ternary T_g is mostly close to or lower than the low T_g of the corresponding binary. The reason for the low T_g is likely because of insufficient hydrogen bonding but still miscible probed by DSC. The ternary T_g values in Fig. 3(c) were found to all lower than the low T_g of the corresponding binary. The reason is similar to those in Fig. 3(b).

Table 6
Glass transition temperatures of PVPh/sPMMA/PVCN blends

	T_g (°C)	ΔT_g (°C)
PVPh/sPMMA/PVCN		
75.4/18.2/6.4	136.1	16
75.9/12.6/12.5	131.7	22
74.8/6.4/18.8	116.4	29
50.1/37.7/12.2	129.5	32
49.9/25.0/25.1	95	9
50.1/12.6/37.3	102.5	19
24.8/56.5/18.7	114.1	11
25.1/37.7/37.2	88.1	15
25.0/18.4/56.6	80.6	15

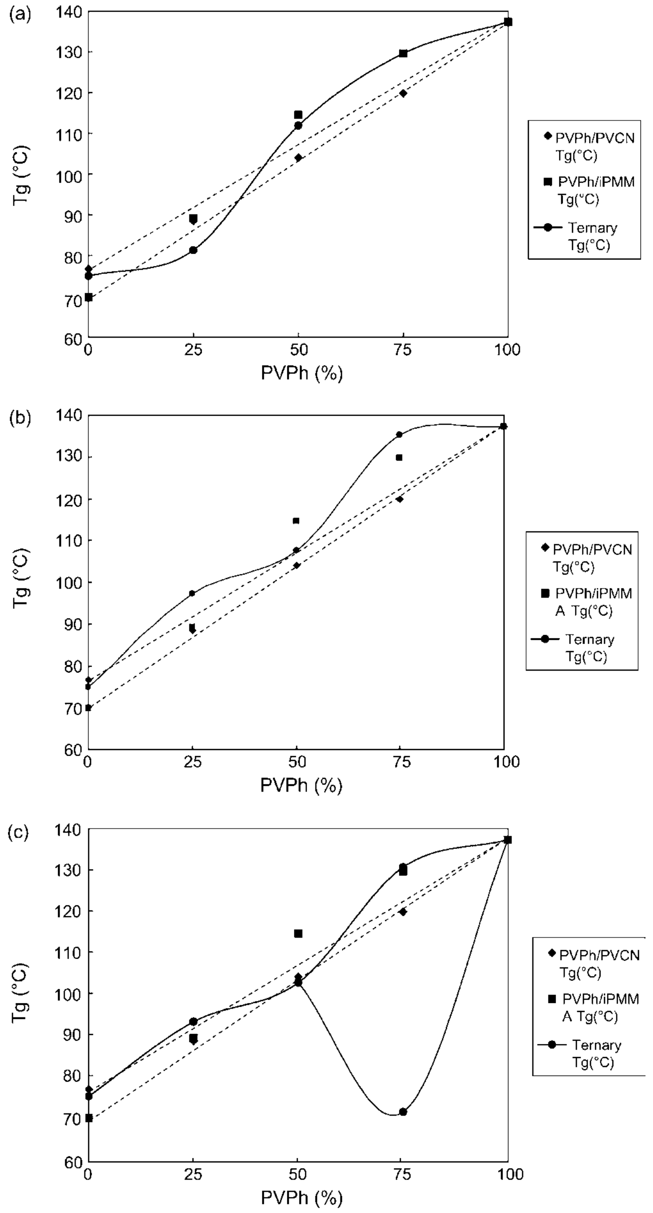

Fig. 2. (a) Change of T_g of the ternary blends with PVPh composition (iPMMA /PVCN weight ratio = 3/1). (●) Data point, (◆) PVPh/PVCN blends, (■) PVPh/iPMMA blends (curves drawn for viewing). (b) Change of T_g of the ternary blends with PVPh composition (iPMMA /PVCN weight ratio = 1/1). (●) Data point, (◆) PVPh/PVCN blends, (■) PVPh/iPMMA blends (curves drawn for viewing). (c) Change of T_g of the ternary blends with PVPh composition (iPMMA /PVCN weight ratio = 1/3). (●) Data point, (◆) PVPh/PVCN blends, (■) PVPh/iPMMA blends (curves drawn for viewing).

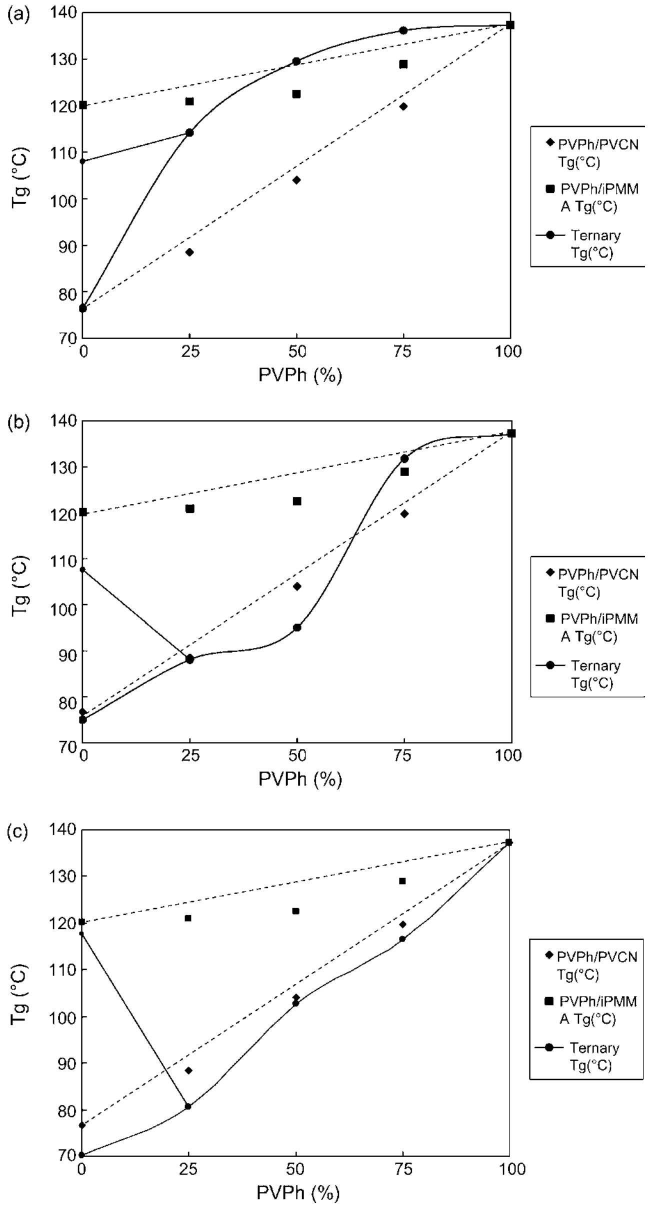

Fig. 3. (a) Change of T_g of the ternary blends with PVPh composition (sPMMA /PVCN weight ratio = 3/1). (●) Data point, (◆) PVPh/PVCN blends, (■) PVPh/sPMMA blends curves drawn for viewing). (b) Change of T_g of the ternary blends with PVPh composition (sPMMA /PVCN weight ratio = 1/1). (●) Data point, (◆) PVPh/PVCN blends, (■) PVPh/sPMMA blends (curves drawn for viewing). (c) Change of T_g of the ternary blends with PVPh composition (sPMMA/PVCN weight ratio = 1/3) (●) data point, (◆) PVPh/PVCN blends, (■) PVPh/sPMMA blends (curves drawn for viewing).

3.5. Phase diagram and Fox equation

Using single T_g as the criterion for miscibility, the phase diagram composed of PVPh, PVCN and PMMA was established and is shown in Figs. 4 and 5 in the order of iPMMA(1), iPMMA and sPMMA, respectively. The solid and empty circles represent single T_g and two T_gs. Miscibility is encountered in the studied PVPh/sPMMA/PVCN blends. However, a small immiscibility region encompassing four empty circles and one empty circle was observed in Fig. 4(a) and (b), respectively. The closed immiscibility loop behavior was similar to a previous study of PVPh/aPMMA/PVCN blends [13]. The reason for iPMMA(1) ternaries to demonstrate larger immiscibility loop than iPMMA ternaries was commented as follows: For PVPh/iPMMA(1)/PVCN ternary, the order of the binary interaction can be arranged (based on the *k* value as an indicator) as PVCN/iPMMA(1) $\gg$ PVPh/iPMMA(1) $\geqq$ PVPh/PVCN. Therefore a large immiscibility region was due to much stronger PVCN/iPMMA(1) interaction than PVPh/iPMMA(1) (or PVPh/PVCN) interaction. For PVPh/iPMMA/PVCN ternary, the

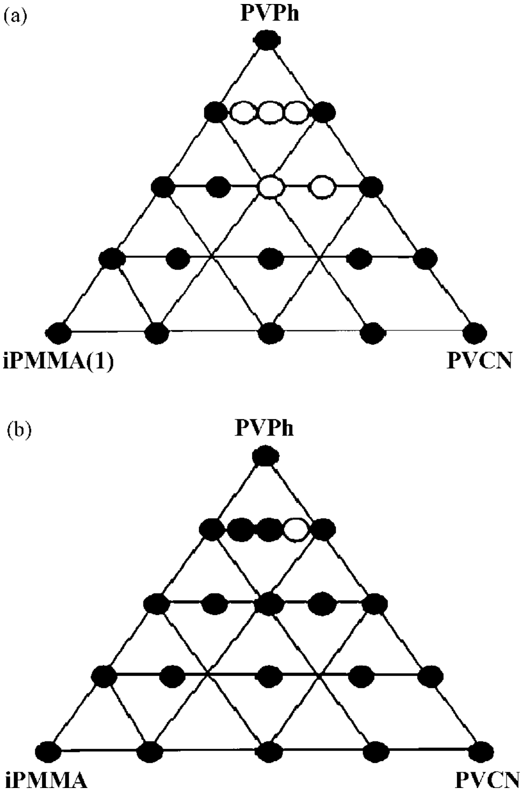

Fig. 4. (a) Phase diagram of PVPh/iPMMA(1)/PVCN ternary blends (●) one T_g, (○) two T_gs. (b) Phase diagram of PVPh/iPMMA/PVCN ternary blends: one T_g, (○) two T_gs.

order of the binary interaction is as PVCN/iPMMA(≒PVPh/iPMMA) > PVPh/PVCN. Because of the matching of two stronger binary interactions, a much smaller immiscibility was detected. Since the interaction parameter of PVCN with PMMA (or PVPh) was not known according to our knowledge. Attempts of fitting the phase diagram by some binary interaction models were not resorted.

PVCN was found to be not miscible with sPMMA. The interaction of PVPh/PVCN is slightly stronger than that of PVPh/sPMMA but likely in similar strength. Therefore a completely miscible region was observed in the sPMMA ternary blends. In comparison with previous study of aPMMA ternaries [13], iPMMA or sPMMA with approximately the same molecular weight as aPMMA was shown mostly to demonstrate miscible behavior when blended with PVPh and PVCN.

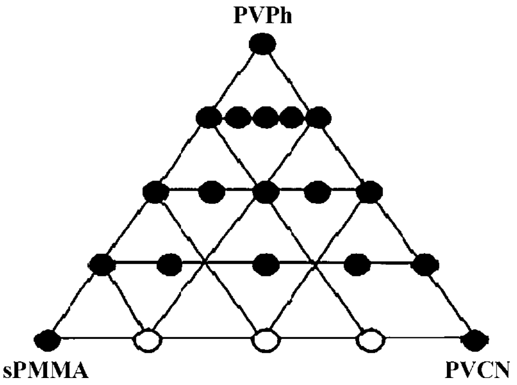

Fig. 5. Phase diagram of PVPh/sPMMA/PVCN ternary blends: one T_g, (○) two T_gs.

Table 7
Glass transition temperatures of PVPh/PMMA/PVCN blends versus Fox predictions

	T_g (°C)	T_{gF} (°C)
PVPh/iPMMA(1)/PVCN		
50.0/37.5/12.5	74.8	90.4
25.1/56.5/18.4	80.2	70.6
25.1/37.9/37.0	81.1	76.7
25.2/18.4/56.4	88.6	84.1
PVPh/iPMMA/PVCN		
75.2/18.6/6.2	129.6	118.7
75.0/12.5/12.5	135.2	119.2
50.0/37.6/12.4	111.9	101.5
49.9/25.3/24.8	107.5	102.9
50.2/12.6/37.2	102.6	104.4
24.7/56.5/18.8	81.3	85.4
25.2/37.8/37.0	97.3	88.0
25.0/18.5/56.5	93.1	89.3
PVPh/sPMMA/PVCN		
75.4/18.2/6.4	136.1	129.6
75.9/12.6/12.5	131.7	126.5
74.8/6.4/18.8	116.4	126.8
50.1/37.7/12.2	129.5	122.4
49.9/25.0/25.1	95	116.1
50.1/12.6/37.3	102.5	110.4
24.8/56.5/18.7	114.1	115.2
25.1/37.7/37.2	88.1	106.6
25.0/18.4/56.6	80.6	97.9

For predicting the miscible ternary T_g, the Fox equation derived for weak or no interaction was used as a qualitative attempt and listed as below [16]

$$\frac{1}{T_g}=\frac{w_1}{T_{g1}}+\frac{w_2}{T_{g2}}+\frac{w_3}{T_{g3}} \qquad (2)$$

where all the symbols have the same meaning as in Eq. (1). The T_{gF} values were estimated using the T_g values of PVPh, PVCN and PMMA (iPMMA(1), iPMMA or sPMMA) in Eq. (2).

The outcome of T_{gF} values is shown in Table 7. The Fox predictions are in qualitative agreement with experimental T_g data. Most experimental T_g values are larger than or approximately equal to Fox estimations likely because of hydrogen bonding in the blends. The ternary blends with T_g higher than T_{gF} often contain high percentage of PVPh composition.

4. Conclusion

When iPMMA or sPMMA was used instead of aPMMA to blend with PVPh and PVCN, a more miscible ternary blend was obtained. The reason for PVPh/iPMMA/PVCN ternaries to demonstrate mostly miscibility was because the PVCN/iPMMA interaction was similar in strength to PVPh/iPMMA interaction. The interaction of PVPh/PVCN is slightly stronger than that of PVPh/sPMMA, therefore a completely miscible region was observed in the PVPh/sPMMA/PVCN ternary blends. For PVPh/iPMMA(1)/PVCN blends, the PVCN/iPMMA(1) interaction is much stronger than the other two binary interactions. A large immiscibility loop of ternary region was therefore observed. In this article, the *k* value of the Gordon–Taylor equation was proven to be a good indicator of binary interaction strength.

Acknowledgment

The financial support by the National Science Council of Taiwan, ROC. NSC94-2216-E-239-005 is highly appreciated.

References

[1] D.R. Paul, in: C.B. Bucknall (Ed.), Polymer Blends, vol. 1/2, John Wiley & Sons, 2002.
[2] O. Olabisi, L.M. Robeson, M.T. Shaw, Polymer–Polymer Miscibility, Academic Press, New York, 1979.
[3] R.L. Scott, J. Chem. Phys. 17 (1949) 279.
[4] H. Tompa, Soc. Faraday Trans. 45 (1949) 1142.
[5] T.K. Kwei, H.L. Frisch, R.W. Radigan, S. Vogel, Macromolecules 10 (1977) 157.
[6] Y.Y. Wang, S.A. Chen, Polym. Eng. Sci. 21 (1981) 47.
[7] D. Rigby, J.L. Lin, R.J. Roe, Macromolecules 18 (1985) 2269.
[8] W.H. Jo, J.Y. Kim, M.S. Lee, J. Polym. Sci. Part B: Polym. Phys. 32 (1994) 1321.
[9] K.E. Min, J.S. Chiou, J.W. Barlow, D.R. Paul, Polymer 28 (1987) 1721.
[10] A. Robard, D. Patterson, G. Delmas, Macromolecules 10 (1977) 706.
[11] C.C. Hsu, J.M. Prausnitz, Macromolecules 7 (1974) 320.
[12] A.C. Su, J.R. Fried, Polym. Eng. Sci. 27 (1987) 1657.
[13] W.P. Hsu, Thermochim. Acta 454 (2007) 50.
[14] W.P. Hsu, J. Appl. Polym. Sci. 86 (2002) 2720.
[15] M. Gordon, J.S. Taylor, J. Appl. Chem. 2 (1952) 493.
[16] T.G. Fox, J. Appl. Bull. Am. Phys. Soc. 1 (1956) 123.